Wide Bandwidth Low Complexity Isolated Current Sensor to be Employed in a 10kW/500kHz Three-Phase Unity Power Factor PWM Rectifier System

Gerold LAIMER
+41-1-632-7447
laimer@lem.ee.ethz.ch

Johann W. KOLAR
+41-1-632-2834
kolar@lem.ee.ethz.ch

Swiss Federal Institute of Technology (ETH) Zurich
Power Electronic Systems Laboratory
ETH-Zentrum/ETL I16 CH-8092 Zurich
SWITZERLAND / Europe

Abstract. A current sensor employing a Hall-based field sensing ASIC in combination with a current transformer is proposed. The sensor is characterized by a measuring range of ±50A, an upper bandwidth limit of 20MHz and high dv/dt-immunity up to 10kV/µs. The sensor functional principle and dimensioning are discussed in detail. Parameters determining the sensor bandwidth are clarified, the theoretical considerations are verified by experiments. Finally, measures for further increasing the sensor bandwidth are proposed.

1 INTRODUCTION

As shown in [1] by application of SiC diodes in combination with latest power MOSFET technology (CoolMOS) the switching frequency of high power three-phase PWM rectifier systems could be increased to 500kHz at high efficiency resulting in a power density of up to 10kW/dm^3. However, the high switching frequency and/or the high switching speed do pose special requirements on the bandwidth and dv/dt-immunity of the phase current sensing used for input current control. Commercially available current sensors which are comprising an AC current transformer and a Hall-based DC and/or low-frequency current transducer in closed-loop (compensating) [2] or open-loop [3] operation show a bandwidth of typ. <200kHz, and do exhibit high frequency output signal oscillations (cf. Fig.9 in [4]) and a relatively large dv/dt-sensitivity (cf. **Fig.1**). Therefore, the sensors cannot be employed in very high switching frequency applications.

In this paper therefore an open-loop current sensor with ±50A measuring range is proposed, which is characterized by a high upper bandwidth limit of 20MHz, high dv/dt-immunity, high linearity and low offset drift and does show a low realization effort.

In **Section 2** the basic functional principle of the sensor is described and measures for minimizing the dv/dt-sensitivity are discussed. In **Section 3** the procedure of dimensioning the sensor is treated in detail. The influence of the number of turns of the secondary and of the current transformer stray inductance on the sensor upper bandwidth limit is shown in **Section 4**. There, furthermore, a sensor upper bandwidth limit of 20MHz is verified experimentally. As the comparison of the sensor output signal to the output of a 50MHz current probe (Tektronix A6302) shows (**Section 5**) the sensor is ideally suited for measuring the input current of high switching frequency PWM rectifier systems.

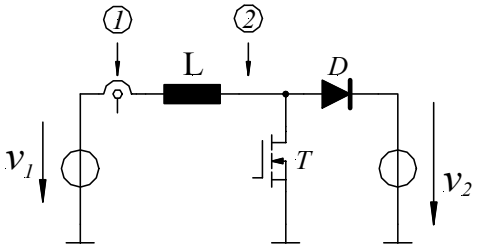

(a)

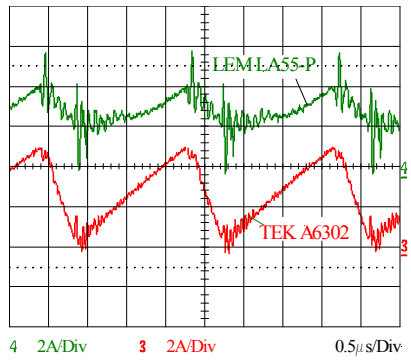

(b)

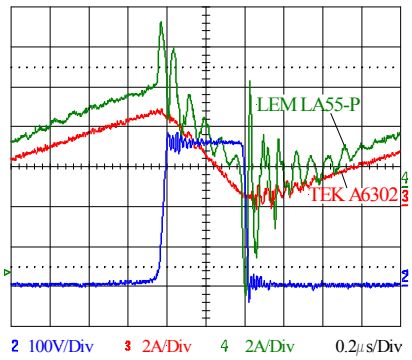

(c)

Fig.1: Testing of a closed-loop/compensating Hall-based current transducer (LEM LA55-P) in a 500kHz DC/DC boost converter **(a)** simulating transducer operating conditions as occurring for input phase current measurement in three-phase PWM rectifier systems; **(b):** LEM LA55-P output signal (upper trace) and actual current time behavior acquired by a 50MHz Tektronix current probe (A6302) for employing the sensor in the connection to the supplying voltage source v_1 (position 1 in (a)); **(c):** LEM LA55-P and A6302 output signal for current measurement at position 2 in (a); furthermore shown: power transistor drain-to-source voltage. Currents in (b) and (c) are shown with equal scales.

Finally, in **Section 6** modifications of the current sensor construction for further increasing the upper bandwidth limit are proposed.

As shown in **Fig.2** for isolated high bandwidth DC and AC current measurement basically magnetoresistive transducers [5] or Hall-effect-based closed-loop or open-loop current transducers could be employed. Transducers based on nonlinear behavior of magnetic materials [6,7] do require complex signal electronics and/or winding arrangements and therefore are not considered in this paper. Also, optical current transducers [7] based on the Faraday-effect which are frequently applied in high-voltage power distribution systems shall not be treated in more detail.

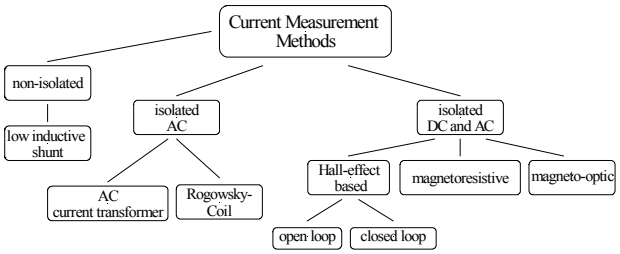

Fig.2: Classification of current measurement principles.

The open loop concept [3] which combines a Hall-element for aquiring low-frequency current components and a passive AC current transformer does show significant advantages concerning manufacturing technology, circuit complexity, and power consumption and therefore will be employed in the following.

1 BASIC CONCEPT OF THE PROPOSED CURRENT SENSOR

The mechanical construction and the circuit schematic of the proposed current sensor are shown in **Fig.3** in combination with an equivalent circuit. A magnetic field sensing ASIC of type Allegro 3515EUA [8] comprising a Hall-element and signal electronics is employed. The integrated circuit provides a highly linear output referenced to +2.5V and features low offset drift and/or high temperature stability. A capacitor of C=100pF at the ASIC output is recommended in the ASIC data sheet. By physical series connection of the AC current transformer output voltage v_2 and of the ASIC output voltage v_m a direct summation of the high-frequency and low frequency (including DC) primary current components is achieved with low realization effort. Also, bandwidth limitations and offset problems which would result for employing a summing operational amplifier are avoided.

The supply voltage of the ASIC advantageously should be used as reference voltage for an A/D-conversion of the sensor output. In this case for varying reference voltage, the A/D converter LSB and/or gain will vary in correspondence to the gain and offset voltage of the ASIC which is proportional to the supplying voltage.

In order to prevent capacitive common-mode currents i_{cm} resulting from dynamic changes of the potential of the primary conductor from flowing into the signal electronics a low impedance path is provided by connecting a capacitor C_{cm}= 10nF from one terminal of the current transformer secondary to ground.

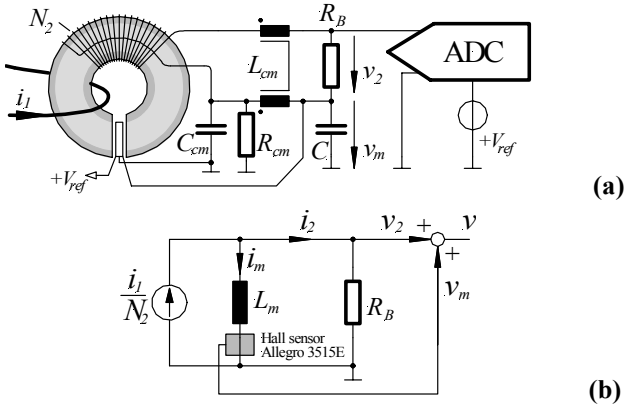

Fig.3: Basic concept **(a)** and equivalent circuit **(b)** of the proposed current sensor. Low frequency components of the current i_1 to be measured are not compensated by the secondary current i_2 of the AC current transformer and are therefore resulting in a finite magnetizing current i_m. As the output signal of the magnetic field sensing Hall-element is proportional to i_m the total primary current i_1 is reconstructed without error by summation $N_2 (i_2 + i_m)$. There, proper scaling of both quantities has to be provided by dimensioning and/or trimming of R_B (or V_{ref}).

Furthermore, a common mode inductor L_{cm} is inserted in between the secondary winding terminals and the burden resistor R_B (cf. **Fig.4**(a)). L_{cm} is realized by a toroidal magnetic core of material T38 and 10 turns. This does constitute a high common mode impedance over a wide frequency range as verified by impedance measurements (cf. Fig.4(b))

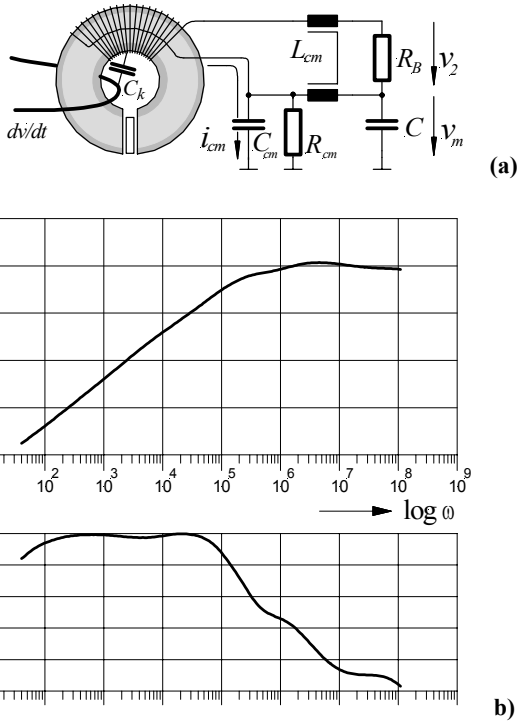

Fig.4: Capacitive common mode current i_{cm} resulting from dynamic changes of the potential of the primary conductor and the parasitic capacitive coupling C_k to the AC current transformer secondary (cf. **(a)**). Furthermore shown: common-mode impedance of L_{cm} **(b)** as recorded by a HP4294 impedance analyzer.

2 DIMENSIONING OF THE MAGNETIC SYSTEM

The current sensor should be designed for application in a 10kW/500kHz three-phase three-level PWM rectifier system in a hard switching mode of operation. There, the sensor does experience a common mode voltage stress of up to 40kV/µs.

The peak input current of the PWM rectifier is ≈30A. Accordingly, the measuring range of the sensor is selected to be ±50A in order to leave enough margin for the sensing of overcurrent conditions. The upper bandwidth limit of the sensor should be as high as possible in order to cope with even more demanding future requirements resulting from further increased switching frequency.
For converting the sensor output into digital form the sensor output voltage range should be matched to the input voltage range of the A/D-converter so that no additional electronic components for adaption are required and minimum circuit complexity is achieved.
As mentioned, the current sensor is comprised by a DC and AC part. The signals of both parts are directly added without using any frequency-matching network.

For acquiring DC and low frequency AC currents with high accuracy an integrated three-terminal Hall-effect device (Allegro 3515E) is employed which features

- linear, ratiometric output
- output signal shifted by half the supply voltage
- single voltage supply in the range of 4.5V to 5.5V (typ. 5.0V)
- dynamic offset cancellation
- internal temperature drift compensation
- precise recoverability after temperature cycling
- high bandwidth (-3dB at 30kHz).

The sensor shows a sensitivity of S_{Hall} = 50mV/mT and does provide a ratiometric rail-to-rail output voltage span.

The input voltage range of the A/D-converter employed (ADS803) is ±2.0V with reference to an offset voltage of 2.5V, i.e. 0A ≡ 2.5V.

For matching the sensor output to the input voltage range of the A/D-converter the current sensor has to be designed properly. A gapped ferrite toroidal core is employed for concentrating the magnetic flux as resulting from the primary current. The minimum gap width is defined by the thickness of to the Hall device package (≈1.57mm). Accordingly, an air gap length of δ=1.6mm is selected which in combination with the sensitivity S_{Hall} of the Hall device directly determines the peak primary current which can be accommodated into the Hall sensor measuring range.

The magnetic flux density B_{gap} in the core resulting from a primary current I_1 is given by

$$B_{gap} = \frac{I_1 \cdot \mu_0}{\delta}. \qquad (1)$$

According to the peak value of the magnetic flux in the air gap the Hall sensor generates an output voltage of

$$\pm\hat{U}_H = S_{Hall} \cdot \pm\hat{B}_{gap}. \qquad (2)$$

where the output voltage swing should be ±2.0V in order to have a matching to the A/D-converter input voltage range.

Using (1) and (2) the peak current value can be calculated as

$$\hat{I}_1 = \frac{\hat{U}_H}{S_{Hall} \cdot \mu_0}\delta = \frac{2.0V}{50\frac{V}{T}\mu_0} \cdot 1.6mm = 50.29A,$$

leading to a sensitivity of the DC current sensing part of

$$S_{DC} = \frac{2.0V}{50.93A} = 39.27\frac{mV}{A}.$$

Widening the air gap would reduce the core flux density, correspondingly the upper limit of the current measuring range would increase. It should be pointed out that the air gap is mandatory also for preventing a saturation of the magnetic core material.

The AC part of the current sensor has to be designed for equal sensitivity as the DC part in order to be able to directly add the individual sensor output signals without employing an adaption network. Furthermore, the low-frequency bandwidth limit f_T of the AC current transformer has to be selected about a decade below the upper bandwidth limit f_H of the Hall sensor.

The sensitivity of the AC current transformer is determined by the number of turns N_2 of the secondary winding and by the burden resistance R_B. In order to achieve a high upper bandwidth limit a low number of secondary turns has to be selected. However, this does result in a high secondary current and/or relatively high losses in the burden resistance. Therefore, a compromise has to be found between N_2 and the resistance value R_B.
The inductance of N_2 turns on a toroidal core with air gap δ is

$$L = \mu_0 \frac{N_2^2}{\delta} \cdot A_{Fe}. \qquad (3)$$

The transformed peak input current value $\pm\hat{1}_1 / N_2$ should result in a voltage across R_B of $\hat{U}_B$ = ±2.0V in order to ensure a sensitivity equal to the DC sensing part. Accordingly, the burden resistance can be calculated as

$$R_B = \frac{N_2}{\hat{i}_1} \cdot \hat{U}_B. \qquad (4)$$

Assuming N_2=70 one receives

$$R_B = \frac{70}{50.93A} \cdot 2.0V = 2.75\Omega. \qquad (5)$$

In order to achieve a low sensor volume we select a toroidal core of type R20/10/7 (EPCOS, material N30) having a cross sectional area of 33.63mm^2. With (3) there results a secondary winding inductance of

$$L = \mu_0 \cdot \frac{70^2}{1.6mm} \cdot 33.36mm = 130\mu H. \qquad (6)$$

The resulting corner frequency is

$$f_T = \frac{R_B}{2\pi L} = \frac{2.75\Omega}{2\pi \cdot 130\mu H} = 3.36kHz \qquad (7)$$

which is well below the upper bandwidth limit f_H of the Hall sensor.

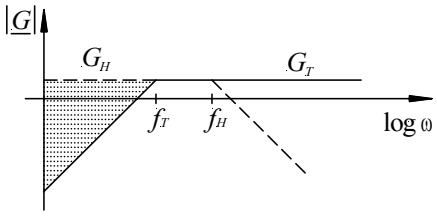

Fig.5: Selection of the frequency response of the AC current transformer G_T with reference to the frequency response and bandwidth of the Hall-element G_H. The low-frequency bandwidth f_T of the current transformer is selected well below the bandwidth f_H of the Hall-element. Therefore, the shape of the frequency response of the Hall-element for frequencies $f > f_T$ is of no importance and a cross-over distortion resulting after summation of the output signals of the current transformer and the Hall-element is prevented. The frequency range to be covered by the Hall-element is pointed out by a dotted area.

3 UPPER BANDWIDTH LIMIT OF THE AC CURRENT TRANSFORMER

The upper bandwidth limit of the current transformer is defined by the characteristic frequency f_2 of the parallel resonance circuit formed by the parasitic capacitance C_2 of the secondary winding and the current transformer stray inductance L_σ, i.e. by $f_2 = (2\pi \sqrt{C_2 L_\sigma})^{-1}$. The capacitance C_2 is mainly determined by the capacitance of the winding to the magnetic core, the influence of capacitances between turns of the single layer winding is comparably low as a large number of turns is connected in series [9,10].

It is interesting to note that f_2 could be considered as first resonance of the short-circuited transmission line formed by the secondary winding. Assuming a relative permittivity of the winding isolation of $\varepsilon_r \approx 5$ and an effective permeability of $\mu_r^* \approx 30$ (cf. **Fig.6**) and considering the total length of $l_2 = 1.75$m of the winding $l_2 = \lambda/4$ is reached for $f \approx 3.7$MHz which is in good agreement with the results of impedance measurements. At $l_2 = \lambda/4$ the short circuit at the output of the transmission line is translated into an input open circuit behavior and/or ideally infinite input impedance (parallel resonance). For $f > f_2$ further parallel and series resonance as being typical for transmission lines do occur. For a detailed calculation of the high frequency impedance characteristic of the secondary, e.g., also the frequency dependency of the permeability and of the losses of the magnetic material would have to be taken into account (cf. [11], p. 65). However, the only immediate measure available for increasing the current transformer bandwidth is a reduction of the number of turns and/or of the length of the secondary winding. This could be verified in Fig.6 by considering the frequency dependency of the winding impedance for different numbers of turns for frequencies in between f_2 and the subsequent series resonance.

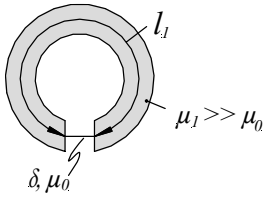

Fig.6: Calculation of the effective permeability of the current transformer magnetic core (cf. p. 38 in [12]). Considering $\mu_1 >> \mu_0$ we have for the effective permeability of a magnetic core without airgap and equal magnetic induction $\mu^* \approx \mu_0 (l_1 + \delta)/\delta$ and/or in the case at hand $\mu_r^* \approx 30$. In combination with $\varepsilon_r \approx 5$ this does result in a propagation of electromagnetic waves with $c = c_0/\sqrt{\varepsilon_r \mu_r^*} \approx 0.086 c_0$ m/s and/or in a wavelength of e.g 2.6m for $f = 10$MHz.

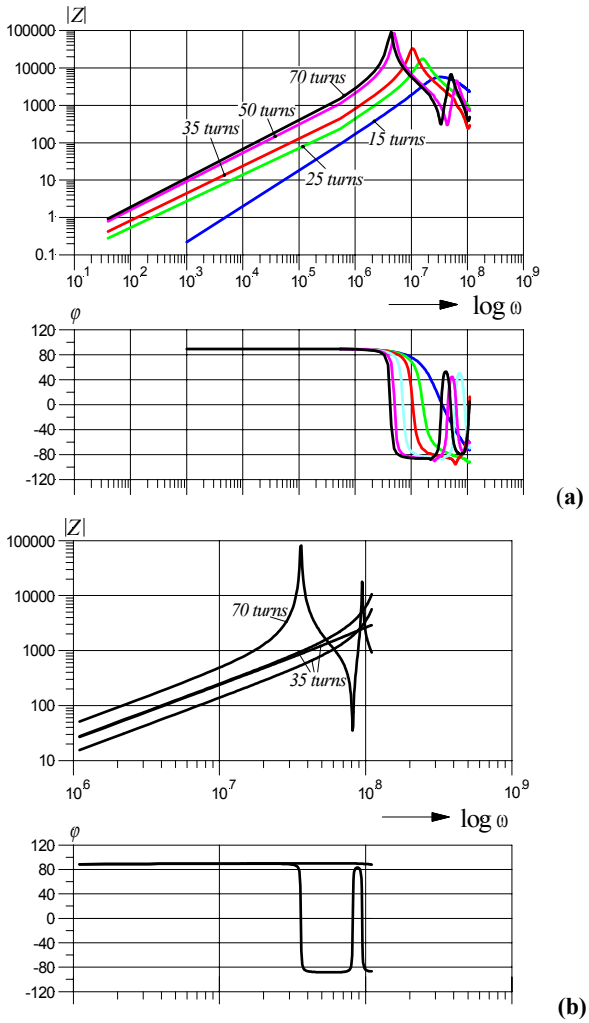

Fig.7: Frequency characteristic **(a)** of the current transformer secondary winding impedance as acquired by impedance analyzer HP4294 for different numbers of turns N_2 and winding arrangements. A damping of the resonances appearing at higher frequencies could be achieved by connecting damping resistors across winding segments. Furthermore show: impedance characteristic **(b)** of a winding on a non-magnetic core (material FR4) of equal dimensions. There, due to $\mu_r = 1$ the first resonance is shifted to higher frequencies and the distance of the parallel and series resonance frequencies is in closer correspondence to transmission line theory (cf. $N_2 = 70$) due to the negligible high frequency losses of the core material.

The resulting normalized transfer function of the final

current sensor construction is shown in **Fig.8**. Amplitude and phase errors remain limited to low values for frequencies up to 20MHz. Furthermore, no noticeable crossover distortion at the transfer from the Hall-element to the AC current transformer does occur.

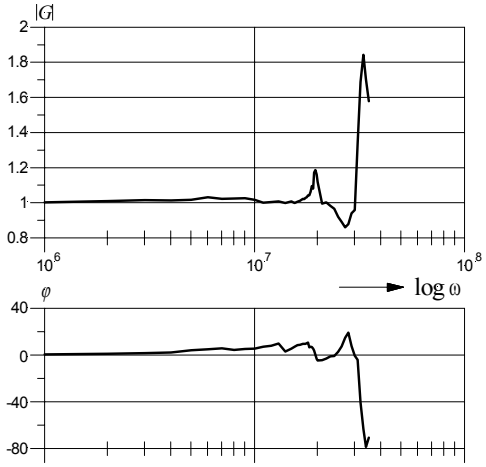

Fig.8: Bode plot of the current sensor transfer function. For connecting the sensor output to the oscilloscope input via a 50Ω coaxial cable a 50Ω termination at the oscilloscope end should be provided. Furthermore, the cable should be connected to the sensor output via a series resistor of $(50\ \Omega - R_B)$ [13].

In order to analyze the influence of the current transformer stray inductance L_σ on the sensor bandwidth L_σ has been artificially increased by an external inductance of L_e = 12µH. As shown in **Fig.9** this does result in considerably decreased current transformer bandwidth and/or does verify the theory.

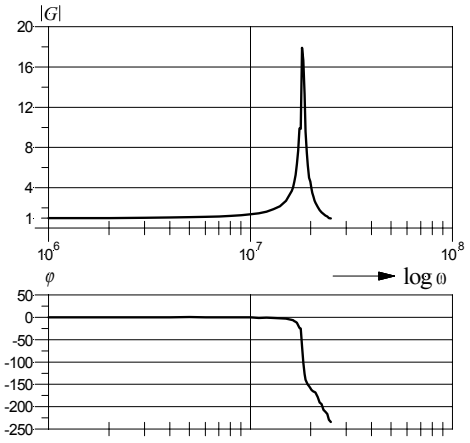

(a)

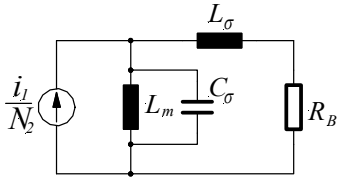

(b)

Fig.9: Bode plot of the current sensor transfer function for artificially increasing the current transformer stray inductance L_σ **(a),(b)** and high frequency equivalent circuit **(c)** of the current transformer. The characteristic frequency $1/(2\pi\sqrt{C_2 L_\sigma})$ of the parallel resonant circuit formed by the parasitic capacitance C_2 of the secondary and L_σ does define the upper bandwidth limit.

4 EXPERIMENTAL RESULTS

Results of an experimental analysis of the proposed current sensor are shown in **Fig.10**. Excellent dynamic behavior and high dv/dt-immunity are achieved despite no shielding of the primary conductor is provided.

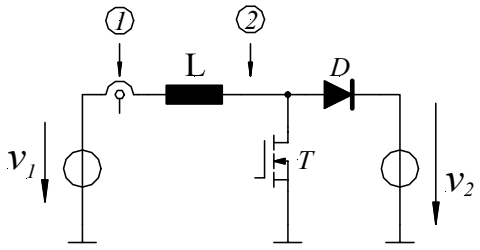

(a)

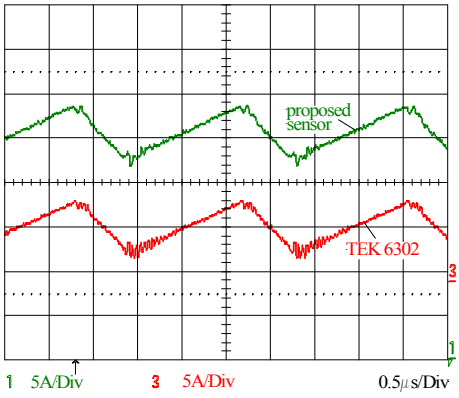

(b)

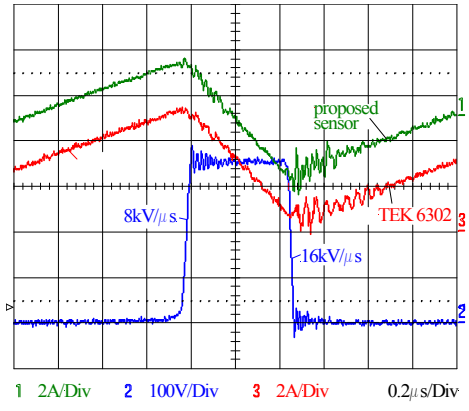

(c)

Fig.10: Testing of the proposed current sensor in a 500kHz DC/DC boost converter **(a)** simulating operating conditions as occurring for input phase current measurement in three-phase PWM rectifier systems; **(b):** sensor output signal (upper trace) and actual current time behavior as acquired by a 50MHz current probe Tektronix A6302 for positioning the sensor in the connection to the supplying voltage source (position 1 in (a)); **(c):** proposed sensor and A6302 output signal for current measurement at position 2 in (a); furthermore shown: power transistor drain-to-source voltage. Currents in (b) and (c) are shown with equal scales.

5 CONCLUSIONS

In this paper a new current sensor (cf. **Fig.11**) which shows wide bandwidth, high dv/dt-immunity and low complexity and therefore is of special interest for applications in future very high switching frequency PWM rectifier systems has been proposed.

As detailed in Section 3 the measuring range of the sensor is determined by the length of the air gap required for accommodating the magnetic field sensing ASIC and has been set to ±50A in the case at hand. Accordingly, changing the measuring range to e.g. ±25A would require a different sensor package (the ASIC does occupy only part of the package volume) or a doubling of the number of primary turns.

In the course of the continuation of the research means for further increasing the sensor bandwidth, as e.g.

- cascading [10] of the proposed sensor and an ungapped AC current transducer and
- splitting the secondary into several partial windings which are decoupled by common-mode inductors [10]

will be analyzed. Experimental results and a comparison to the performance of the conventional sensor construction will be published at a future conference.

Fig.11: Prototype of the proposed current sensor.

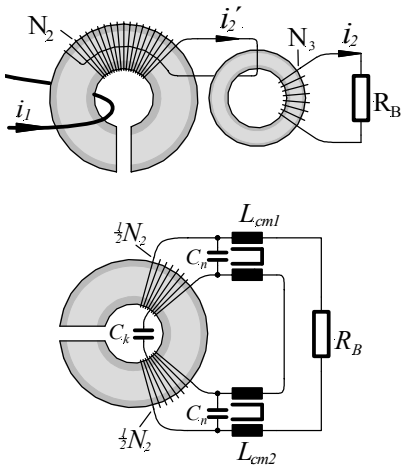

Fig.12: Cascading of current sensors (**a**) and partitioning of the current transformer secondary **(b)** in order to reduce the number of turns and/or the parasitic winding capacitance impairing the high frequency sensor behavior. A partitioning of the secondary winding into n=6 partial windings is e.g. employed in current probes of type Tektronix A6303; there, in order to deactivate the total winding capacitance each partial winding could be terminated by R_B/n (e.g. employed in Pearson current transformers) or common-mode inductors have to be provided which do suppress a current flow via the total winding capacitance C_2 so that just the partial winding capacitances C_n are effective.

REFERENCES

[1] **Laimer, G., and Kolar, J.W.:** *Accurate Measurement of the Switching Losses of Ultra High Switching Speed CoolMOS Power Transistor-SiC Diode Combination Employed in Unity Power Factor PWM Rectifier Systems.* To be published at the International Conference on Power Conversion, Intelligent Motion and Power Quality, May 14-16, Nuremberg, Germany (2002).

[2] **Friot, M.:** *Towards the Ideal Current Transducer.* PCIM Europe, No. 6, pp. 316-318 (1997).

[3] **Rollier, S., Huber, H.D., and Richard, B.:** *New Solutions for Current Measurements.* Power Electronics Europe, No. 4, pp. 13 – 16 (2001).

[4] **Pankau, J., Leggate, D., Schlegel, D., Kerkman, R., and Skibinski, G.:** *High Frequency Modeling of Current Sensors.* Proceedings of the 14th IEEE Applied Power Electronics Conference, Dallas (TX), USA, March 14-18, Vol. 2, pp. 788-794 (1999).

[5] http://www.sensitec.de/strom.html

[6] **Undeland, T.M.:** *Low Cost DC and AC Current Transducer with Isolation and Good Linearity*. Proceedings of the 4th Annual International Power Conversion Conference, March 29-31, San Francisco, USA, pp. 341-353 (1982).

[7] **Pejovic, P.:** *Circuits for Direct Current Measurement with Improved Linearity and Accuracy.* Record of the 7th European Power Electronics Conference, Trondheim, Norway, Sept. 8-10, Vol. 3, pp. 3.288-3.293 (1997).

[8] http://www.allegromicro.com/

[9] **Costa, F., Laboure, E., and Gautier, C.:** *Wide Bandwidth Large AC Current Probe for Power Electronics and EMI Measurements.* IEEE Transactions on Industrial Electronics, Vol. 44, No. 4, pp. 502 – 511 (1997).

[10] **Laboure, E., Costa, F., and Forest, F.:** *Current Measurement in Static Converters and Realization of a High Frequency Passive Current Probe (50A-300MHz).* Record of the 5th European Power Electronics Conference, Brighton, UK, Sept. 13 – 16, Vol. 4, pp. 478-483 (1993).

[11] http://www.epcos.de/inf/80/db/fer_01/00310106.pdf

[12] **Feldtkeller, R.:** Theorie der Spulen und Übertrager (in German). 5th Edition, ISBN-Nr. 3 7776 0243 4, S. Hirzel Verlag, Stuttgart, 1971.

[14] **Cordingley, B.V.:** *Wideband Terminated Current Transformers for Power Electronic Measurements.* Proceedings of the 7th International Conference on Power Electronics and Variable Speed Drives, London, UK, Sept. 21-23, pp. 433-436 (1998).